

Cite this: *Chem. Sci.*, 2025, 16, 147

All publication charges for this article have been paid for by the Royal Society of Chemistry

Donor-free 9,10-dihydro-9,10-dialuminaanthracenes†

Paula L. Lückert, Jannik Gilmer, Alexander Virovets, Hans-Wolfram Lerner and Matthias Wagner*

Despite their promising potential, e.g., as ditopic, cooperatively binding Lewis acids, 9,10-dihydro-9,10-dialuminaanthracenes (DAA-R₂; R: terminal Al-bonded substituent) have remained unexplored for long due to the challenges in synthesizing the ligand-free species. We demonstrate that DAA-Me₂ is accessible via the reaction of 1,2-(Me₃Sn)₂C₆H₄ with AlMe₃, producing volatile SnMe₄ as the sole byproduct. In non-coordinating solvents and in the solid state, DAA-Me₂ exists as a dimer (DAA-Me₂)₂. Treatment of (DAA-Me₂)₂ with 4 equiv. AlBr₃ cleaves the dimer, leads to quantitative Me/Br exchange, and forms the double AlBr₃ adduct DAA-Br₂·(AlBr₃)₂. Removal of AlBr₃ with 2,2'-bipyridine gives free DAA-Br₂, which also dimerizes in the absence of bases to form (DAA-Br₂)₂. (DAA-Me₂)₂ and (DAA-Br₂)₂ readily react with mono- (e.g., pyridine) or ditopic Lewis bases (e.g., potassium pyrazolide) to afford *trans*-diadducts or triptycene-type frameworks. Upon addition of [nBu₄N]Br, DAA-Br₂·(AlBr₃)₂ undergoes selective cleavage of Al–C bonds to produce the Br[−] chelate complex of 1,2-(Br₂Al)₂C₆H₄, a valuable synthon for 1,2-dideprotonated benzenes.

Received 12th October 2024
Accepted 16th November 2024

DOI: 10.1039/d4sc06940d

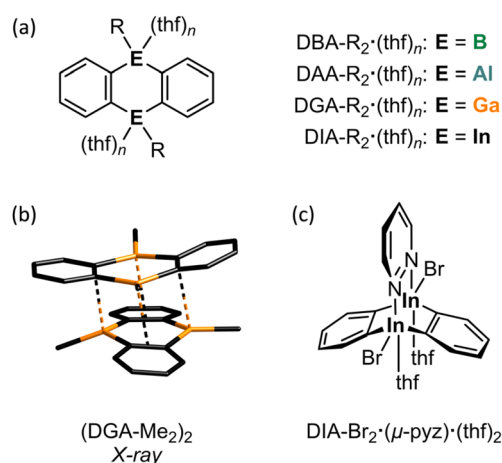
rsc.li/chemical-science

Introduction

The incorporation of p-block elements other than carbon into polycyclic aromatic hydrocarbons ('heteroatom doping') has emerged as a powerful tool for imparting new and valuable chemical and physical properties to these compounds.¹ Notable examples are 9,10-dihydro-9,10-diboraanthracenes (DBAs; Fig. 1a, E = B), which have found wide-ranging applications,² including their use as fluorophores³ or homogeneous catalysts.⁴ To further enhance the utility of DBAs, various substituted derivatives have been developed,^{5,6} the B-doped acene scaffold has been expanded by benzannulation,⁷ and additional heteroatoms (such as N, O, and S) have been introduced into the delocalized π system.⁸

Significantly less attention has been given to what is arguably the most impactful modification: the exchange of the B atoms for their higher homologues.^{9,10} While a few anthracenes containing Al (DAAs),^{11,12} Ga (DGAs),^{11,13} or In (DIAs)^{11,14–18} at the 9,10-positions are known, these compounds are typically isolated as their Lewis-base adducts, which inherently diminishes the desired reactivity. As an example, the synthesis of DAA-Me₂·(thf)_n according to Bickelhaupt *et al.*¹¹ uses MeAlCl₂

(ref. 19) and [Mg(thf)(*o*-C₆H₄)]₄, prepared from [Hg(*o*-C₆H₄)]₃,^{20,21} in THF;^{11,22} DGA-Me₂·(thf)_n and DIA-Me₂·(thf)_n were synthesized in a similar manner (Fig. 1a, E = Al, Ga, or In; n ≥ 2).¹¹ The solubility requirements of the Mg²⁺ reagent necessitate the use of THF, which inevitably precludes the formation of ligand-free heteroanthracenes. Also in the synthesis of the octafluorinated congener of DAA-Me₂·(thf)_n, where 1,2-(Me₃Sn)₂C₆F₄ and Me₂AlCl are employed as starting materials, the cyclocondensation of the initially formed intermediate into the target product must be



Institut für Anorganische und Analytische Chemie, Goethe-Universität Frankfurt, Max-von-Laue-Straße 7, D-60438 Frankfurt (Main), Germany. E-mail: matthias.wagner@chemie.uni-frankfurt.de

† Electronic supplementary information (ESI) available: Synthetic procedures, NMR spectra, X-ray crystallographic data and computational details. CCDC 2385628–2385640. For ESI and crystallographic data in CIF or other electronic format see DOI: <https://doi.org/10.1039/d4sc06940d>

Fig. 1 (a) General structures of thf adducts of heteroanthracenes (E = B, Al, Ga, or In). (b) Solid-state structure of (DGA-Me₂)₂ with all H atoms omitted for clarity. (c) Triptycene-type structure of DIA-Br₂·(μ-pyz)·(thf)₂, where pyz = pyridazine.



initiated by adding THF.¹² Donor-free DGA-R₂ is accessible from 1,2-(ClHg)₂C₆H₄ and GaR₃ in *p*-xylene (R = Me, Et; 140 °C, 3 h).¹³ This protocol, however, poses considerable risks due to the toxic or pyrophoric precursors and particularly the extremely harmful byproduct HgR₂, which is released in 4 equivalents. DGA-R₂ dimerizes *via* Ga...π interactions or Ga-C_b-Ga two-electron three-center bonds (2e3c; C_b: bridging C atom),²³ with (DGA-Me₂)₂ (Fig. 1b) and (DGA-Et₂)₂ having distinctly different molecular structures in the solid state (see below).

Moving on to In offers novel perspectives for several reasons: (i) due to the 'inert-pair effect', In(i) halides are more stable and easier to handle than their Al(i) or Ga(i) counterparts. Consequently, [Hg(*o*-C₆H₄)₃] in THF can conveniently be reacted with InBr in a combined transmetallation/redox reaction to furnish DIA-Br₂·(thf)₄ and elemental Hg, which is a significantly less concerning byproduct compared to HgMe₂ mentioned earlier.¹⁴ (ii) Due to its larger atomic radius, each In site in DIA-Br₂ can accommodate two Lewis bases within a trigonal-bipyramidal ligand sphere, instead of just one. Given the increasing significance of coordination networks and microporous solids,^{24,25} it is noteworthy that DIA-Br₂·(thf)₄, when combined with rigid, ditopic Lewis bases such as 1,4-diazine, has been used to self-assemble molecular stairs and ladders.¹⁶ When 1,2-diazine (pyridazine, pyz) is offered to DIA-Br₂·(thf)₄ instead of 1,4-diazine, the system switches to a chelating mode, leading to the formation of a triptycene-type structure DIA-Br₂·(μ-pyz)·(thf)₂ (Fig. 1c).¹⁷ This outcome points to the potential application of DIA-Br₂·(thf)₄ as a homogeneous Lewis acid catalyst with cooperating heteroatoms.¹⁸

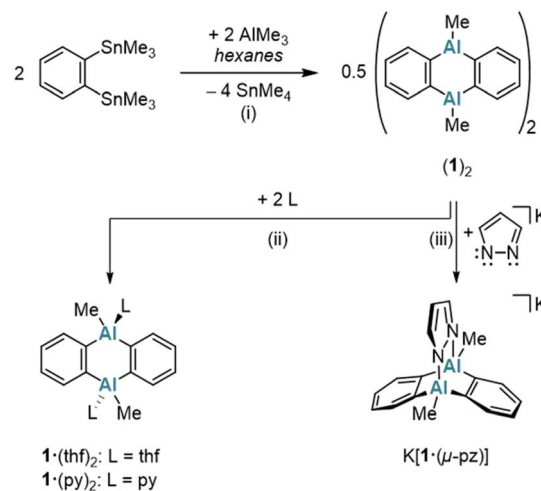
Herein, we present efficient access routes to the first donor-free 9,10-dihydro-9,10-dialuminaanthracenes (DAA-Me₂)₂, (1)₂, and (DAA-Br₂)₂, (2)₂, which exist as dimers in non-coordinating solvents and in the solid state. We further describe selective reactions of (1)₂ and (2)₂ with (i) mono- and bidentate N- or O-Lewis bases and (ii) the Lewis acid AlBr₃.¹⁹ Beyond their intriguing electronic structures, these compounds hold promise as preorganized, ditopic Lewis acids²⁶ and rare *ortho*-dimetallated benzene building blocks for organic synthesis.

Results and discussion

Syntheses

A classical protocol for the synthesis of DBA-X₂ is based on reactions between 1,2-(Me₃E)₂C₆H₄ and BX₃ in toluene, *n*-hexane, or under solvent-free conditions (E = Si, Sn; X = Cl, Br).^{3a,d,5} To extend this approach to the synthesis of DAAs with the aim to avoid the use of [Hg(*o*-C₆H₄)₃] and coordinating solvents, we explored whether 1,2-(Me₃E)₂C₆H₄ could also serve as a suitable *o*-phenylene source in the present case. Eisch *et al.* reported that the reaction of the corresponding stannane with AlCl₃ in toluene gives 1,2-(Cl₂Al)₂C₆H₄.²⁷ However, a serious drawback is that the Me₃SnCl byproduct remains firmly complexed with the aryl alane, resulting in an inseparable polymeric ion pair. Although using AlMe₂Cl somewhat mitigated this issue – yielding a weaker electron-pair acceptor in 1,2-(Me₂Al)₂C₆H₄ – the Me₃SnCl could still not be completely removed.²⁷ Considering modified approaches, we noted that the tetrafluoro

species 1,2-(Me₃Sn)₂C₆H₄ reacts with Me₂AlCl to form dimeric [1,2-(Cl(Me)Al)₂C₆F₄]₂ and SnMe₄ (rather than Me₃SnCl).²⁸ This suggested that starting with AlMe₃ (ref. 19) could prevent the formation of difficult-to-remove chlorostannanes altogether. Indeed, when 1,2-(Me₃Sn)₂C₆H₄ (ref. 29) is treated with an equimolar amount of AlMe₃ in hexanes at elevated temperatures (150 °C, 3 d, sealed glass ampoule), SnMe₄ is released and cyclocondensation to the heteroanthracene occurs (Scheme 1). The dimeric product (1)₂ precipitates in pure form from the reaction mixture upon cooling to room temperature (yield: 76%); (1)₂ is highly soluble in C₆H₆, toluene, CHCl₃, or CH₂Cl₂. The volatile byproduct SnMe₄ can be easily removed and, in principle, subjected to a redistribution reaction with SnCl₄ to regenerate³⁰ the Me₃SnCl required for the synthesis of the starting material 1,2-(Me₃Sn)₂C₆H₄. In the presence of Lewis-basic ligands such as tetrahydrofuran (THF) or pyridine (py), (1)₂ is cleaved into the monomers, which are obtained as the diadducts 1·(thf)₂ (ref. 11) and 1·(py)₂ (Scheme 1). Of particular interest is the coordination behavior of 1 toward bidentate ligands, as this reveals the potential of 1 as a preorganized, ditopic Lewis acid. Initial exploratory investigations with pyridazine (pyz) led to the following observations: (i) the room-temperature ¹H NMR spectrum of an equimolar mixture of (1)₂ and pyz in THF-*d*₈ showed only minor changes of ± 0.03 ppm compared to the chemical shift values of the signals of 1·(thf)₂ and free pyz. (ii) Upon gas-phase diffusion of *n*-hexane into such mixtures, however, the heteroadduct 1·(pyz)(thf) crystallized, which features a pyz ligand that coordinates to one Al site through one of its N atoms, while a thf ligand coordinates to the other Al site (Fig. S41†).^{16,31} In contrast, the boron and indium congeners DBA-H₂ and DIA-Br₂ show triptycene-type structures with E-(μ-pyz*)₂-E' moieties

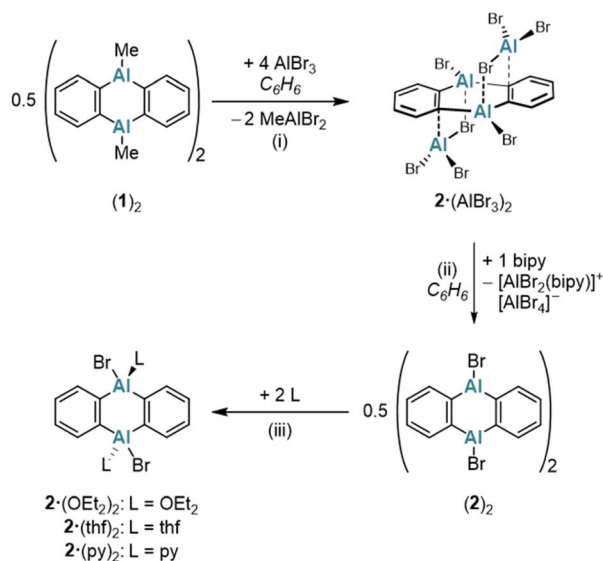


Scheme 1 The Sn/Al exchange reaction of 1,2-(Me₃Sn)₂C₆H₄ with AlMe₃ leads to the formation of donor-free (1)₂. In the presence of Lewis bases (THF or py), (1)₂ is cleaved into the monomeric diadducts 1·(thf)₂ or 1·(py)₂. The heterotriptycene K[1·(μ-pz)] is synthesized by reacting (1)₂ with Kpz. (i) Hexanes, 150 °C, 3 d, sealed glass ampoule. (ii) 1·(thf)₂: in THF, room temperature; 1·(py)₂: 2.1 equiv. py, C₆H₆, room temperature. (iii) 1 equiv. Kpz, THF, room temperature.

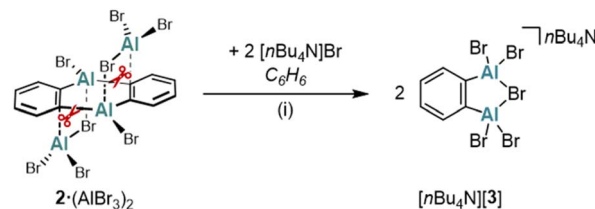


under comparable conditions in the solid state ($E = B, In; \text{pyz}^* = \text{benzo}[d]\text{pyridazine}$).^{17,32} A THF-stable heterotriptycene motif can also be imposed on **1** by using the negatively charged, five-membered pyrazolato ($[\text{pz}]^-$) ligand instead of the neutral, six-membered pyz ligand (*cf.* $\text{K}[1 \cdot (\mu\text{-pz})]$; Scheme 1).

To expand the variety of donor-free DAAs, it would be desirable to obtain also an Al-halogenated derivative DAA- X_2 . One possibility is to start from (**1**)₂ and to achieve the necessary Me/X exchange by the reaction with AlX_3 . AlBr_3 was selected for this purpose because, unlike AlCl_3 , it is soluble in the non-coordinating solvent C_6H_6 . Treatment of (**1**)₂ in C_6H_6 with 8 equiv. AlBr_3 leads to the instantaneous precipitation of $2 \cdot (\text{AlBr}_3)_2$, which is generally poorly soluble in non-coordinating solvents (Scheme 2). If only 4 equiv. AlBr_3 per (**1**)₂ are used instead of 8 equiv., a structure similar to $2 \cdot (\text{AlBr}_3)_2$ is obtained, but with the non-bridging Br positions partially occupied by Me groups [$\text{DAA-R}_2 \cdot (\text{AlBr}_2)_2$; $R = \text{Me}$ or Br ; according to X-ray crystallography, Fig. S42†]. Having achieved the aimed-for Me/Br exchange on **1**, the next task is to remove the two coordinating AlBr_3 molecules from $2 \cdot (\text{AlBr}_3)_2$ to obtain the free heteroanthracene. The chelating ligand 2,2'-bipyridine (bipy) proved to be ideally suited for this purpose: In C_6H_6 , the addition of 1 equiv. bipy to $2 \cdot (\text{AlBr}_3)_2$ resulted in the formation of (**2**)₂ after heating and sonication. NMR spectroscopy on the supernatant revealed exclusively signals of the free, dimeric (**2**)₂, with no detectable bipy resonances (Scheme 2). We assume that the solid consists of species such as $[\text{AlBr}_2(\text{bipy})][\text{AlBr}_4]$, which, due to their salt-like nature, quantitatively separate from the target product.³³ Similar to (**1**)₂, (**2**)₂ is converted to $2 \cdot (\text{OEt}_2)_2$,



Scheme 2 The addition of AlBr_3 to (**1**)₂ results in the immediate precipitation of $2 \cdot (\text{AlBr}_3)_2$. Donor-free (**2**)₂ is formed by the reaction of $2 \cdot (\text{AlBr}_3)_2$ with bipy. In the presence of Lewis-bases (Et_2O , THF, or py), (**2**)₂ is cleaved into the monomeric diadducts $2 \cdot (\text{OEt}_2)_2$, $2 \cdot (\text{thf})_2$, or $2 \cdot (\text{py})_2$. (i) 4 equiv. AlBr_3 per monomeric unit **1**, C_6H_6 , room temperature, 1 d. (ii) 1 equiv. bipy, C_6H_6 , 70 °C, 2 h, sonication. (iii) $2 \cdot (\text{OEt}_2)_2$: exc. Et_2O , C_6H_6 , room temperature; $2 \cdot (\text{thf})_2$: 2.1 equiv. THF, C_6H_6 , room temperature; $2 \cdot (\text{py})_2$: 2.1 equiv. py, C_6H_6 , room temperature.



Scheme 3 The reaction of $2 \cdot (\text{AlBr}_3)_2$ with $[n\text{Bu}_4\text{N}]\text{Br}$ yields the 1,2-dialumino-substituted benzene derivative $[n\text{Bu}_4\text{N}][\text{3}]$. (i) 2 equiv. $[n\text{Bu}_4\text{N}]\text{Br}$, C_6H_6 , 70 °C, 1.5 h, sonication.

$2 \cdot (\text{thf})_2$, or $2 \cdot (\text{py})_2$ upon addition of Et_2O , THF, or py, respectively (Scheme 2).

In another attempt to generate the AlBr_3 -free (**2**)₂, Br^- ions were used as alternative ligands instead of bipy. However, the reaction between $[n\text{Bu}_4\text{N}]\text{Br}$ (2 equiv.) and $2 \cdot (\text{AlBr}_3)_2$ in C_6H_6 furnished the 1,2-dialumino-substituted benzene derivative $[n\text{Bu}_4\text{N}][\text{3}]$, rather than the initially expected products (**2**)₂ and $[n\text{Bu}_4\text{N}][\text{AlBr}_4]$ (Scheme 3). Formally, $2 \cdot (\text{AlBr}_3)_2$ is a dimer of 1,2- $(\text{Br}_2\text{Al})_2\text{C}_6\text{H}_4$, and $[\text{3}]^-$ is the Br^- adduct of this ditopic, chelating Lewis acid (a comparable F^- adduct of the boron-based ditopic Lewis acid 1,2- $[(\text{C}_6\text{F}_5)_2\text{B}]_2\text{C}_6\text{F}_4$ has been characterized by NMR spectroscopy).³⁴

Solid-state structures

Note: Whenever we want to indicate individual DAA units in a molecular structure, we will hereafter use dashed lines for any interactions between a respective unit and the rest of the molecule. This is not intended to imply any judgements about the nature or strength of the interaction.

The crystal of (**2**)₂ is a true racemate of discrete chiral C_2 -symmetric units, best described as dimers of DAA- Br_2 molecules (Fig. 2a; note that the corresponding B-doped DBA- Br_2 is monomeric in the solid state³⁴).³⁵ The Al_2C_4 cores of the individual monomers adopt distorted, shallow boat conformations [dihedral angles $\text{Al}(1)\text{C}(1)\text{C}(7)//\text{C}(1)\text{C}(2)\text{C}(7)\text{C}(8) = 35.3(2)^\circ$, $\text{Al}(2)\text{C}(2)\text{C}(8)//\text{C}(1)\text{C}(2)\text{C}(7)\text{C}(8) = 6.0(2)^\circ$]. The Al atoms of monomer M (or M') interact with two C(*ipso*) atoms, both bonded to the same Al atom of monomer M' (or M), as schematically depicted in Fig. 3a. The corresponding bond lengths $\text{Al}(1')\text{-C}(2)$ and $\text{Al}(2')\text{-C}(8)$ measure 2.261(3) and 2.191(3) Å, respectively; the angles including these Al-C bonds and the $\text{C}(2)\cdots\text{C}(5)$ or $\text{C}(8)\cdots\text{C}(11)$ vectors across the corresponding phenylene rings are $\text{Al}(1')\text{-C}(2)\cdots\text{C}(5) = 101.9(1)$ and $\text{Al}(2')\text{-C}(8)\cdots\text{C}(11) = 111.6(2)^\circ$. In summary, (**2**)₂ forms a cage structure with six-membered rings serving as the base and top, and one four-membered, two five-membered, and one six-membered ring(s) constituting the belt (Fig. S44 and S45†). To facilitate the analysis of $\text{M}\cdots\text{M}'$ interactions in (**2**)₂, we assume that each bridging C_b is sp^2 -hybridized, neglecting contributions from Wheland-type³⁶ electronic structures with sp^3 -hybridized C_b atoms. Within this model, an Al' atom from monomer M' can engage with monomer M either through the unhybridized p_z orbital of C_b ($\text{Al}'\cdots\pi(\text{Ar})$ interaction) or *via* the $\text{Al}\text{-C}_b$ σ bond (to generate a $2e3c$ bond). Of the four $\text{M}\cdots\text{M}'$ interactions present



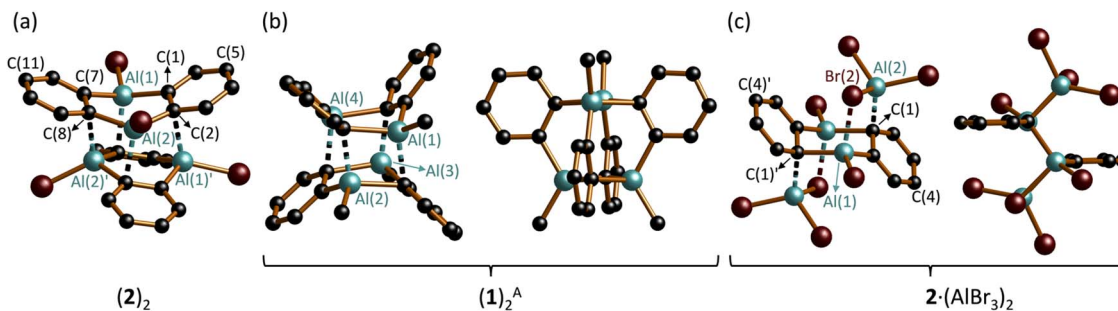


Fig. 2 Molecular structures in the solid state: (a) $(2)_2$; (b) $(1)_2^A$ viewed as a dimer of DAA monomers M, M' (left) and as a tetramer of equivalent $C_6H_4-Al(Me)$ fragments (right); (c) $2 \cdot (AlBr_3)_2$ shown as a $AlBr_3$ diadduct of $DAA-Br_2$ (left) and viewed from the side (right). H atoms omitted for clarity. C: black, Br: brown, Al: turquoise.

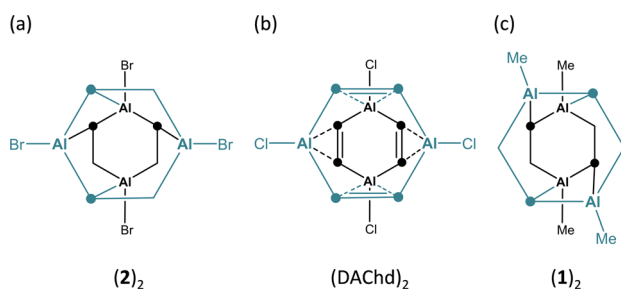


Fig. 3 Schematic representations to illustrate the intermonomer contacts in (a) $(2)_2$, (b) $(DACHd)_2$, and (c) $(1)_2$.

in $(2)_2$, two are pairwise identical. Intrinsic bond orbitals (IBOs) of the remaining two distinct interaction types are illustrated in Fig. S52.† Both types have contributions from $Al \cdots \pi(Ar)$ and $2e3c$ interactions, but to varying degrees: Based on the interpretation of IBOs, Wiberg bond indices (WBIs), and Mayer bond orders (MBOs), the two $M \cdots M'$ interactions within the four-membered ring of the belt appear to be dominated by $2e3c$ bonding, whereas the other two intermonomer bonds are predominantly of the $Al \cdots \pi(Ar)$ type (Fig. S52 and S53†). $(2)_2$ can be compared with the dimeric 1,4-dichloro-2,3,5,6-tetramethyl-1,4-dialumina-2,5-cyclohexadiene [(DACHd) $_2$], where the two non-planar monomers are rotated by 90° relative to each other and are linked *via* four $Al \cdots \pi(olefin)$ bonds (Fig. 3b). The distance between two Al atoms of different monomers within the same dimer is about 3.00 \AA , which was regarded as 'relatively short'; according to *ab initio* calculations, $Al \cdots Al'$ interactions contribute to the stability of the system.³⁷ Indeed, the dimers remained intact under mass spectrometry conditions up to temperatures of $140 \text{ }^\circ\text{C}$.³⁸ In $(2)_2$, the $Al \cdots Al'$ distances range from $2.717(2) \text{ \AA}$ (across the four-membered ring) to $3.635(2) \text{ \AA}$ (across the six-membered ring). A third dimeric structural motif comparable to $(2)_2$ and $(DACHd)_2$ is observed in $(DGA-Me_2)_2$ (Fig. 1b): the primary distinction among these three cases lies in the degree of rotation of the monomer units relative to each other.¹³

$(1)_2$ crystallizes with three crystallographically independent molecules in the unit cell, each displaying approximate D_{2d} symmetry [$(1)_2^A - (1)_2^C$].³⁹ Since their key structural parameters

are very similar (Fig. S35†), only $(1)_2^A$ will be discussed in detail. Although its molecular formula corresponds to a dimer of $DAA-Me_2$, the assignment of two distinct DAA units within the total ensemble is less unambiguous than in the case of $(2)_2$, owing to the higher symmetry of $(1)_2^A$. For the purposes of the discussion to follow, the six-membered rings containing $Al(1)/Al(4)$ and $Al(2)/Al(3)$ are defined as belonging to monomers M and M' (Fig. 2b, left; an alternative definition is possible but leads to the same conclusions). Both monomeric units exhibit twist-boat conformations. Unlike $(2)_2$, the Al atoms of monomer M (or M') in $(1)_2^A$ interact with two diagonally opposite C(*ipso*) atoms attached to different Al atoms of monomer M' (or M) (*cf.* Fig. 3c). The respective 'intermonomeric' Al-C bond lengths range from $2.100(2)$ to $2.132(2) \text{ \AA}$, which are shorter than those of $(2)_2$. While these findings are informative for the comparison of the solid-state structures of $(1)_2$ and $(2)_2$, an alternative analysis of the $(1)_2$ scaffold is more appropriate to account for its high symmetry: the cluster comprises four equivalent $C_6H_4-Al(Me)$ fragments, each featuring a $C(Ar)-Al$ σ bond; the second deprotonated *o*-phenylene C atom bridges two additional Al atoms, forming an $Al'-C_b-Al''$ $2e3c$ bond (Fig. 2b, right). Consequently, each Al vertex is tetracoordinated by C atoms. The Al_4 core of $(1)_2$ adopts a strongly distorted tetrahedral geometry with $Al \cdots Al$ distances of av. 2.666 and av. 3.611 \AA . Overall, the framework of $(1)_2$ resembles that of $(DGA-Et_2)_2$ (ref. 13) and of the *o*-phenylene magnesium tetramer $[Mg(thf)(o-C_6H_4)]_4$, with the Al atoms replaced by Mg atoms and the Me substituents by thf ligands (Fig. S36 and S37†).²¹ To conclude the discussion of structures $(1)_2$ and $(2)_2$, we find it remarkable that both species prefer to form discrete dimers in a cluster-like arrangement rather than coordination polymers with $Al-(\mu-Me/Br)_2-Al'$ bridges, as seen in Al_2Me_6 (ref. 40) and Al_2Br_6 ;⁴¹ the diboranthracene $(DBA-H_2)_\infty$ is indeed polymeric *via* $B-(\mu-H)_2-B'$ linkages in the solid state.⁴² Furthermore, it is worth noting the following result from quantum chemical calculations (SMD(C_6H_6)/ ω B97XD/def2-TZVPP//SMD(C_6H_6)/ ω B97XD/def2-TZVPP): after Me/Br or Br/Me exchange, the resulting $(1^{Br})_2$ or $(2^{Me})_2$ remain minima on the potential-energy surface. For R = Me, the crystallographically observed structure $(1)_2$ is more stable than $(2^{Me})_2$ by $4.9 \text{ kcal mol}^{-1}$. Yet, for R = Br, structure $(2)_2$ is less stable than $(1^{Br})_2$ by $3.5 \text{ kcal mol}^{-1}$, in the absence of crystal-packing effects.⁴³



In the C_i -symmetric compound $2 \cdot (\text{AlBr}_3)_2$, two AlBr_3 moieties coordinate to opposite sides of the DAA-Br_2 core, which consequently adopts a chair conformation (Fig. 2c).⁴⁴ Similar to $(1)_2$, the binding sites are two diagonally opposite $C(\textit{ipso})$ atoms (*cf.* Fig. 3c). The respective bonds are relatively short ($\text{Al}(2)-\text{C}(1) = 2.032(4) \text{ \AA}$), and the $C(1)$ atoms are strongly pyramidalized ($\text{Al}(2)-\text{C}(1) \cdots \text{C}(4) = 134.0(2)^\circ$, $\text{Al}(1)-\text{C}(1') \cdots \text{C}(4') = 124.0(2)^\circ$). Each $\text{Al}(2)-\text{C}(1)$ bond is reinforced by a Br atom that bridges the Al atoms of DAA-Br_2 and AlBr_3 ($\text{Al}(1)-\text{Br}(2) = 2.449(1) \text{ \AA}$, $\text{Al}(2)-\text{Br}(2) = 2.411(1) \text{ \AA}$). In summary, the largely symmetric $\text{Al}(1) \cdots \text{Al}(1')$ -bridging mode of the phenylene ring in $2 \cdot (\text{AlBr}_3)_2$ more closely resembles the situation in $(1)_2^A$ than in $(2)_2$. Compound $2 \cdot (\text{AlBr}_3)_2$ is formally the dimer of $1,2-(\text{Br}_2\text{Al})_2\text{C}_6\text{H}_4$. The related $[1,2-(\text{Cl}(\text{Me})\text{Al})_2\text{C}_6\text{F}_4]_2$, which was characterized by Gabbai *et al.* with X-ray diffraction, has a markedly different molecular structure: It features two stacked 1,2-phenylene rings, two distinct types of $\text{Al} \cdots \text{Al}'$ -bridging Cl^- ions, and lacks any $\text{Al}-\text{C}_b-\text{Al}$ 2e3c bonds.²⁸

The compound $[n\text{Bu}_4\text{N}][3]$ is asymmetric in the solid state, although the anionic component approximates the C_{2v} point group (Fig. 4a). $[3]^-$ can be described as a ditopic Lewis acid (*i.e.*, $1,2-(\text{Br}_2\text{Al})_2\text{C}_6\text{H}_4$), where the two vicinally positioned Al sites cooperate in bonding to the same Br^- anion, with an average bond length of $\text{Al}-(\mu\text{-Br}) = 2.443 \text{ \AA}$. As expected, these bonds are longer than the $\text{Al}-\text{Br}$ bonds to the terminal Br atoms, which range from $2.282(2)$ to $2.294(2) \text{ \AA}$. When the bridging Br^- ion is excluded from consideration, the sum of angles within the remaining CAlBr_2 fragments averages 343.7° , which lies between the typical values of a planar (360°) and a tetrahedral geometry (328.5°). The endocyclic angles $(\mu\text{-Br})-\text{Al}-\text{C}$ and $\text{Al}-(\mu\text{-Br})-\text{Al}$ are *av.* 101.8° and $90.7(1)^\circ$, respectively.

In the crystal lattice, $[\text{K}(\text{thf})_{1.5}][1 \cdot (\mu\text{-pz})]$ forms a one-dimensional coordination polymer, with $[\text{K}(\text{thf})]^+$ and $[\text{K}(\text{thf})_2]^+$ cations bonding simultaneously to phenylene rings of two different anions (Fig. S40[†]). The anion $[1 \cdot (\mu\text{-pz})]^-$ represents a rare heterotriptycene with Al atoms at the bridgehead positions (Fig. 4b).^{45–47} The $\text{Al}-\text{N}$ bonds to the bridging pyrazolato ($[\text{pz}]^-$) ring (*av.* 1.973 \AA) are longer than the $\text{Al}-\text{N}(\text{pz})$ bonds in $[\text{R}_2\text{Al}-(\mu\text{-pz})_2-\text{AlR}_2]$ ($\text{R} = \text{Me}$: *av.* 1.921 \AA , $t\text{Bu}$: *av.* 1.929 \AA)⁴⁸ or in bicyclic $[\text{HAL}(\mu\text{-}3,5\text{-}t\text{Bu}_2\text{pz})_2(\mu\text{-CH}_2\text{N}t\text{Bu})\text{AlH}]$ (*av.* 1.914 \AA).⁴⁵

The monomeric complexes $1 \cdot (\text{py})_2 \times \text{C}_6\text{H}_6$ and $2 \cdot (\text{py})_2 \times \text{C}_6\text{H}_6$ are isostructural in the crystalline state and show planar, C_i -symmetric DAA-R_2 units coordinated by two py ligands from

opposite sides (*trans* configuration; $\text{R} = \text{Br}, \text{Me}$). Also, the thf diadducts $1 \cdot (\text{thf})_2$ and $2 \cdot (\text{thf})_2$ adopt *trans* configurations. Remarkably, the OEt_2 ligands in the corresponding diadduct $2 \cdot (\text{OEt}_2)_2$ are positioned in a *cis* arrangement in the solid state (full details are given in the ESI[†]).

NMR analysis

For all molecules presented in this work, the ^{27}Al NMR resonances were broadened beyond detection. NMR spectroscopic analysis was not possible for $2 \cdot (\text{AlBr}_3)_2$ and $[n\text{Bu}_4\text{N}][3]$, due to their low solubility in all suitable solvents. In the cases of the $\text{Et}_2\text{O}/\text{thf}/\text{py}$ diadducts of **1** and **2** as well as $[\text{K}[1 \cdot (\mu\text{-pz})]]$ and $(1)_2$, the number of ^1H and ^{13}C NMR signals, their chemical shift values, and the integral ratios of the proton resonances were consistent with the (symmetry-averaged) molecular structures determined by X-ray analysis (full details are given in the ESI[†]). $(2)_2$ is the only example that requires a more thorough consideration: Its solid-state structure has insufficient symmetry to align with the ^1H and ^{13}C NMR spectra obtained in solution (C_6D_6), which show only two and three signals, respectively. There are two possible explanations for the observed NMR features: (i) $(2)_2$ may dissociate in solution into the monomeric units **2**. (ii) The dimeric structure may persist but experience significant fluctuations due to librational motion of the monomers relative to each other, resulting in an average D_{2d} symmetry. A quantum-chemical analysis renders the conversion of $(2)_2 \rightarrow 2 \times 2$ unlikely, as it would be endergonic with $\Delta G = 28.0 \text{ kcal mol}^{-1}$ (which is in line with the shortened $\text{Al} \cdots \text{Al}'$ distances discussed in the crystallographic section). In contrast, any activation barrier to be overcome during the librational motion does not exceed $\Delta G^\ddagger = 3.0 \text{ kcal mol}^{-1}$ (Scheme S1[†]), which makes option (ii) more probable.

Potential of $[n\text{Bu}_4\text{N}][3]$ as synthesis equivalent of the 1,2-dideprotonated benzene nucleophile

The arylaluminum species described here, while interesting in their own right, also hold potential as *ortho*-dimetallated starting materials for organic synthesis. Such nucleophilic building blocks, which complement their ubiquitous, polarity inverted *o*-dihalogenated analogues, are just as valuable as they are difficult to access.⁴⁹ A major challenge is to avoid the unwanted formation of benzyne on the way to $1,2\text{-M}_2\text{C}_6\text{H}_4$ ($\text{M} = \text{Li}, \text{MgBr}$). The key starting material for most *o*-dimetallated benzenes therefore still remains *o*-phenylene mercury, $[\text{Hg}(o\text{-C}_6\text{H}_4)]_3$, which is obtained from $1,2\text{-Br}_2\text{C}_6\text{H}_4$ and sodium amalgam in a process that takes several days.^{50,51} $[\text{Hg}(o\text{-C}_6\text{H}_4)]_3$ can subsequently be converted into the organolithium, -magnesium, or -zinc species $1,2\text{-Li}_2\text{C}_6\text{H}_4$, $[\text{Mg}(\text{thf})(o\text{-C}_6\text{H}_4)]_4$, or $[\text{Zn}(\text{thf})_2(o\text{-C}_6\text{H}_4)]_n$ [$n = 2$ (crystalline state) or 3 (solution)] by reaction with metallic Li,^{50,52} Mg,²¹ or Zn,⁵³ respectively; the required reaction times range from half a day to weeks. Taken together, the widespread use of *o*-dimetallated benzenes is hindered not only by the well-recognized environmental and health concerns associated with organomercury compounds but also by the apparently poor reproducibility in the synthesis of $[\text{Hg}(o\text{-C}_6\text{H}_4)]_3$: while Wittig claimed to have obtained yields of 50%,

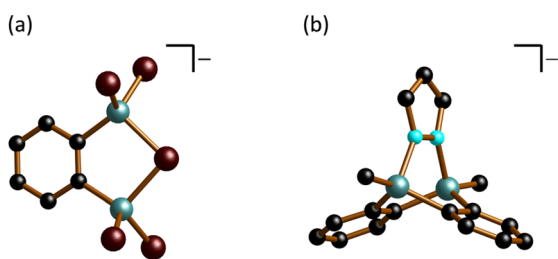
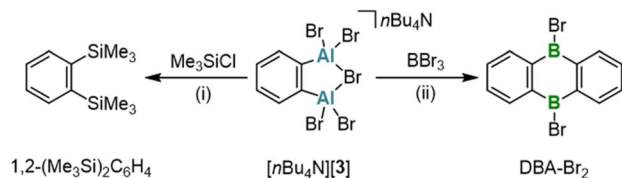


Fig. 4 Molecular structures in the solid state: (a) $[n\text{Bu}_4\text{N}][3]$; (b) $[\text{K}(\text{thf})_{1.5}][1 \cdot (\mu\text{-pz})]$. Counter cations and H atoms omitted for clarity. C: black, Br: brown, Al: turquoise, N: cyan.





Scheme 4 Synthesis of 1,2-(Me₃Si)₂C₆H₄ or DBA-Br₂ by the reaction of [nBu₄N][3] and Me₃SiCl or BBr₃, respectively. (i) 2 equiv. Me₃SiCl, C₆D₆, room temperature, 1 d. (ii) Excess BBr₃, room temperature.

Massey explicitly stated that, despite '10 years of experience in the field', they consistently observed yields as low as 1–2%.^{50,51} Even though, in favorable cases, the *in situ* generation of nucleophilic intermediates from 1,2-Br₂C₆H₄ and Mg can be achieved in the presence of the electrophile, resulting in satisfactory yields (as demonstrated in the synthesis of 1,2-(Me₃Sn)₂C₆H₄),²⁹ there is a persistent demand for efficient access to additional *o*-dimetallated benzenes.

Recognizing the potential of our aryl aluminium compound [nBu₄N][3] as an ideal candidate to address this need, we conducted several proof-of-concept experiments. For this purpose, we selected target compounds with published synthesis protocols that require prolonged reaction times and/or high temperatures (Scheme 4). This allows us to identify potential advantages of our new starting material through direct comparison: For instance, the reaction between [nBu₄N][3] and 2 equiv. Me₃SiCl in C₆D₆ furnished the disubstituted benzene 1,2-(Me₃Si)₂C₆H₄ at room temperature after 1 d (quantitative conversion according to NMR spectroscopy; Fig. S25†). In contrast, the established synthesis of the same product from 1,2-Br₂C₆H₄, Mg, and Me₃SiCl *via* a Grignard-type reaction in THF requires stirring for 2 d, with the temperature gradually increasing from 0 °C to room temperature.⁵⁴ Particularly noteworthy is the conversion of [nBu₄N][3] with neat BBr₃, which instantaneously affords the corresponding 9,10-dihydro-9,10-diboraanthracene already at room temperature (Scheme 4). The traditional route to DBA-Br₂ *via* 1,2-(Me₃Si)₂C₆H₄ and BBr₃ requires heating to 120 °C for 6 d.^{34,55}

Already this selection of straightforward conversions highlights the potential of [3][−] as a synthetic equivalent of 1,2-dideprotonated benzene. Despite its poor solubility in non-polar solvents like C₆H₆, it still undergoes smooth heterogeneous reactions. The products, however, are nicely soluble in C₆H₆, allowing for easy separation from any unreacted starting material and Al-containing byproduct salts, which greatly simplifies the purification process.

Conclusions

Anthracenes incorporating Group 13 elements at the 9,10-positions have significant potential as redox-active systems and versatile ditopic Lewis acids, offering a broad range of applications. Their planar structures expose the reactive heteroatom sites, while the rigid 1,2-phenylene bridges bring these sites into close proximity, promoting acid–base binding cooperativity. Additionally, the delocalized π systems enable

electronic communication between the dopant atoms. While 9,10-dihydro-9,10-diboraanthracenes have been extensively studied and higher homologues have received some attention, 9,10-dihydro-9,10-dialuminaanthracenes (DAA-R₂; R: terminal Al-bonded substituent) have remained almost entirely unexplored, despite Al being by far the most earth-abundant Group 13 element.

In this work, we synthesized DAA-Me₂ (1) in the absence of stabilizing ligands, resulting in its dimerization through Al⋯π(Ar) interactions to form (1)₂. Despite dimerization, (1)₂ serves as an effective synthesis equivalent for 'free' DAA-Me₂, as it readily reacts with mono- or bidentate Lewis bases to afford *trans*-diadducts such as 1⋅(py)₂, or triptycene-type structures like K[1⋅(μ-pz)] (py: pyridine; Hpz: pyrazole). Notably, (1)₂ can be cleaved into its monomers not only by Lewis bases but also by the strong Lewis acid AlBr₃, which displaces the original DAA-Me₂ partner by establishing new Br₃Al⋯π(Ar) bonds and Al–Br–Al' bridges in its place. This reaction also exchanges all Al-bonded Me substituents of DAA-Me₂ for Br atoms, leading to 2⋅(AlBr₃)₂, the double AlBr₃ adduct of DAA-Br₂ (2), which can also be viewed as a dimer of 1,2-(Br₂Al)₂C₆H₄. The donor-free (2)₂ can be liberated from 2⋅(AlBr₃)₂ using 2,2'-bipyridine. In contrast, treatment of 2⋅(AlBr₃)₂ with Br[−] ions splits two Al–C bonds to give the adduct [nBu₄N][3], in which one molecule of 1,2-(Br₂Al)₂C₆H₄ chelates one Br[−] ion. The anion [3][−] has proven to be an excellent synthon for a 1,2-dideprotonated benzene. Such compounds are rare but of exceptional synthetic value; the broader utility of [3][−] in this regard is currently under investigation in our laboratories.

Data availability

The datasets supporting this article have been uploaded as part of the ESI.†

Author contributions

P. L. L. performed the experimental studies and characterized all new compounds. P. L. L. and J. G. performed the quantum-chemical calculations. A. V. performed the X-ray crystal structure analyses of all compounds. H.-W. L. and M. W. supervised the project. The manuscript was written by P. L. L. and M. W. and edited by all co-authors.

Conflicts of interest

There are no conflicts to declare.

Acknowledgements

The authors are grateful to Felipe Fantuzzi (University of Kent) and Eugenia Peresypkina (University of Frankfurt) for helpful discussions. We thank the center for scientific computing (CSC) Frankfurt and the University of Kent for providing HPC resources that contributed to the computational investigation of this work. We acknowledge Liselotte Michels (University of Würzburg) and the microanalytical laboratory Pascher for the elemental analyses.



Notes and references

- 1 (a) A. Borissov, Y. K. Maurya, L. Moshniaha, W.-S. Wong, M. Żyła-Karwowska and M. Stępień, *Chem. Rev.*, 2022, **122**, 565–788; (b) M. Stępień, E. Gońka, M. Żyła and N. Sprutta, *Chem. Rev.*, 2017, **117**, 3479–3716; (c) L. Ji, S. Griesbeck and T. B. Marder, *Chem. Sci.*, 2017, **8**, 846–863.
- 2 (a) S. E. Prey and M. Wagner, *Adv. Synth. Catal.*, 2021, **363**, 2290–2309; (b) E. von Grotthuss, A. John, T. Kaese and M. Wagner, *Asian J. Org. Chem.*, 2018, **7**, 37–53; (c) L. Schweighauser and H. A. Wegner, *Chem.–Eur. J.*, 2016, **22**, 14094–14103.
- 3 (a) E. Januszewski, A. Lorbach, R. Grewal, M. Bolte, J. W. Bats, H.-W. Lerner and M. Wagner, *Chem.–Eur. J.*, 2011, **17**, 12696–12705; (b) E. Januszewski, M. Bolte, H.-W. Lerner and M. Wagner, *Organometallics*, 2012, **31**, 8420–8425; (c) C. Hoffend, F. Schödel, M. Bolte, H.-W. Lerner and M. Wagner, *Chem.–Eur. J.*, 2012, **18**, 15394–15405; (d) C. Reus, S. Weidlich, M. Bolte, H.-W. Lerner and M. Wagner, *J. Am. Chem. Soc.*, 2013, **135**, 12892–12907; (e) C. Reus, F. Guo, A. John, M. Winhold, H.-W. Lerner, F. Jäkle and M. Wagner, *Macromolecules*, 2014, **47**, 3727–3735.
- 4 Selected examples of neutral DBA catalysts: (a) S. N. Kessler and H. A. Wegner, *Org. Lett.*, 2010, **12**, 4062–4065; (b) S. N. Kessler and H. A. Wegner, *Org. Lett.*, 2012, **14**, 3268–3271; (c) S. N. Kessler, M. Neuburger and H. A. Wegner, *J. Am. Chem. Soc.*, 2012, **134**, 17885–17888; (d) L. Schweighauser, I. Bodoky, S. N. Kessler, D. Häussinger, C. Donsbach and H. A. Wegner, *Org. Lett.*, 2016, **18**, 1330–1333; (e) L. Hong, S. Ahles, M. A. Strauss, C. Logemann and H. A. Wegner, *Org. Chem. Front.*, 2017, **4**, 871–875; (f) S. Ahles, J. Ruhl, M. A. Strauss and H. A. Wegner, *Org. Lett.*, 2019, **21**, 3927–3930; (g) S. Beeck, S. Ahles and H. A. Wegner, *Chem.–Eur. J.*, 2022, **28**, e202104085. Selected examples of dianionic [DBA]²⁻ catalysts/element–element bond activators: (h) A. Lorbach, M. Bolte, H.-W. Lerner and M. Wagner, *Organometallics*, 2010, **29**, 5762–5765; (i) E. von Grotthuss, M. Diefenbach, M. Bolte, H.-W. Lerner, M. C. Holthausen and M. Wagner, *Angew. Chem., Int. Ed.*, 2016, **55**, 14067–14071; (j) E. von Grotthuss, S. E. Prey, M. Bolte, H.-W. Lerner and M. Wagner, *Angew. Chem., Int. Ed.*, 2018, **57**, 16491–16495; (k) E. von Grotthuss, S. E. Prey, M. Bolte, H.-W. Lerner and M. Wagner, *J. Am. Chem. Soc.*, 2019, **141**, 6082–6091; (l) H. Budy, S. E. Prey, C. D. Buch, M. Bolte, H.-W. Lerner and M. Wagner, *Chem. Commun.*, 2022, **58**, 254–257; (m) S. E. Prey, C. Herok, F. Fantuzzi, M. Bolte, H.-W. Lerner, B. Engels and M. Wagner, *Chem. Sci.*, 2023, **14**, 849–860.
- 5 S. Brend'amour, J. Gilmer, M. Bolte, H.-W. Lerner and M. Wagner, *Chem.–Eur. J.*, 2018, **24**, 16910–16918.
- 6 (a) T. Jin, M. Bolte, H.-W. Lerner and M. Wagner, *Org. Chem. Front.*, 2022, **9**, 5611–5616; (b) T. Jin, M. Bolte, H.-W. Lerner, J.-M. Mewes and M. Wagner, *Chem.–Eur. J.*, 2022, **28**, e202202234; (c) M. Metzler, M. Bolte, A. Virovets, H.-W. Lerner and M. Wagner, *Org. Lett.*, 2023, **25**, 5827–5832.
- 7 (a) S. Kirschner, J.-M. Mewes, M. Bolte, H.-W. Lerner, A. Dreuw and M. Wagner, *Chem.–Eur. J.*, 2017, **23**, 5104–5116; (b) A. John, M. Bolte, H.-W. Lerner and M. Wagner, *Angew. Chem., Int. Ed.*, 2017, **56**, 5588–5592; (c) A. John, M. Bolte, H.-W. Lerner, G. Meng, S. Wang, T. Peng and M. Wagner, *J. Mater. Chem. C*, 2018, **6**, 10881–10887; (d) A. John, S. Kirschner, M. K. Fengel, M. Bolte, H.-W. Lerner and M. Wagner, *Dalton Trans.*, 2019, **48**, 1871–1877; (e) S. Kirschner, I. Uecker, M. Bolte, H.-W. Lerner and M. Wagner, *Organometallics*, 2019, **38**, 2818–2823; (f) J. Jovaišaitė, S. Kirschner, S. Raišys, G. Kreiza, P. Baronas, S. Juršėnas and M. Wagner, *Angew. Chem., Int. Ed.*, 2023, **62**, e202215071.
- 8 (a) T. Kaehler, M. Bolte, H.-W. Lerner and M. Wagner, *Angew. Chem., Int. Ed.*, 2019, **58**, 11379–11384; (b) T. Jin, L. Kunze, S. Breimaier, M. Bolte, H.-W. Lerner, F. Jäkle, R. F. Winter, M. Braun, J.-M. Mewes and M. Wagner, *J. Am. Chem. Soc.*, 2022, **144**, 13704–13716; (c) M. Metzler, A. Virovets, H.-W. Lerner and M. Wagner, *J. Am. Chem. Soc.*, 2023, **145**, 23824–23831.
- 9 M. Melaimi and F. P. Gabbaï, *Adv. Organomet. Chem.*, 2005, **53**, 61–99.
- 10 M. Oishi, Product Subclass 9: Triorganoaluminum Compounds, in *Science of Synthesis*, ed. H. Yamamoto, Georg Thieme Verlag KG, Stuttgart, 2004, pp. 261–385.
- 11 M. A. Dam, T. Nijbacker, F. J. J. de Kanter, O. S. Akkerman, F. Bickelhaupt and A. L. Spek, *Organometallics*, 1999, **18**, 1706–1709.
- 12 M. Tschinkl, T. M. Cocker, R. E. Bachman, R. E. Taylor and F. P. Gabbaï, *J. Organomet. Chem.*, 2000, **604**, 132–136.
- 13 P. Jutzi, H. Sielemann, B. Neumann and H.-G. Stammer, *Inorg. Chim. Acta*, 2005, **358**, 4208–4216.
- 14 F. P. Gabbaï, A. Schier, J. Riede and D. Schichl, *Organometallics*, 1996, **15**, 4119–4121.
- 15 M. A. Dam, T. Nijbacker, B. C. de Pater, F. J. J. de Kanter, O. S. Akkerman, F. Bickelhaupt, W. J. J. Smeets and A. L. Spek, *Organometallics*, 1997, **16**, 511–512.
- 16 F. P. Gabbaï, A. Schier and J. Riede, *Angew. Chem., Int. Ed.*, 1998, **37**, 622–624.
- 17 F. P. Gabbaï, A. Schier, J. Riede and M. J. Hynes, *Chem. Commun.*, 1998, 897–898.
- 18 M. Tschinkl, A. Schier, J. Riede and F. P. Gabbaï, *Inorg. Chem.*, 1998, **37**, 5097–5101.
- 19 We are aware that the compounds AlMe₃, AlBr₃, and MeAlCl₂ are monomeric neither in solution nor in the solid state. However, for simplicity, the monomeric forms were used in calculating the quantities employed.
- 20 The literature presents contradicting information regarding the degree of association of [Hg(*o*-C₆H₄)]_n: Wittig and Bickelhaupt have proposed values of *n* = 6 (or 4) based on calotte model inspections and molecular weight determinations in solution (ref. 50). Massey *et al.* reported that *n* equals 3 (ref. 51). We will adopt a value of *n* = 3 throughout, as it is supported by the results of single-crystal X-ray structure analyses and mass spectrometric investigations: (a) C. M. Woodard, G. Hughes and A. G. Massey, *J. Organomet. Chem.*, 1976, **112**, 9–19; (b)



- D. S. Brown, A. G. Massey and D. A. Wickens, *Acta Crystallogr., Sect. B: Struct. Crystallogr. Cryst. Chem.*, 1978, **34**, 1695–1697; (c) D. S. Brown, A. G. Massey and D. A. Wickens, *Inorg. Chim. Acta*, 1980, **44**, 193–194.
- 21 (a) M. A. G. M. Tinga, O. S. Akkerman, F. Bickelhaupt, E. Horn and A. L. Spek, *J. Am. Chem. Soc.*, 1991, **113**, 3604–3605; (b) M. A. G. M. Tinga, G. Schat, O. S. Akkerman, F. Bickelhaupt, E. Horn, H. Kooijman, W. J. J. Smeets and A. L. Spek, *J. Am. Chem. Soc.*, 1993, **115**, 2808–2817.
- 22 This study focuses exclusively on heteroanthracenes that lack substituents on the phenylene rings. Substituents attached to Al/Ga/In are denoted after the hyphen; for example, DAA-Me₂ refers to a 9,10-dihydro-9,10-dialuminaanthracene with methyl substituents at the Al sites. The type and number of coordinated Lewis-basic ligands (if present) are added in parentheses.
- 23 One example of a corresponding B–C_b–B 2e3c bond has been crystallographically characterized: A. Hübner, M. Diefenbach, M. Bolte, H.-W. Lerner, M. C. Holthausen and M. Wagner, *Angew. Chem., Int. Ed.*, 2012, **51**, 12514–12518.
- 24 C. Janiak, *Angew. Chem., Int. Ed.*, 1997, **36**, 1431–1434.
- 25 X. Zheng, M. Kato, Y. Uemura, D. Matsumura, I. Yagi, K. Takahashi, S. Noro and T. Nakamura, *Inorg. Chem.*, 2023, **62**, 1257–1263.
- 26 A. Y. Timoshkin, *Chem.–Eur. J.*, 2024, **30**, e202302457.
- 27 J. J. Eisch, K. Mackenzie, H. Windisch and C. Krüger, *Eur. J. Inorg. Chem.*, 1999, 153–162.
- 28 (a) M. Tschinkl, R. E. Bachman and F. P. Gabbaï, *Chem. Commun.*, 1999, 1367–1368; (b) For a more recent example of a similar reaction, see: P. Federmann, R. Müller, F. Beckmann, C. Lau, B. Cula, M. Kaupp and C. Limberg, *Chem.–Eur. J.*, 2022, **28**, e202200404.
- 29 J. J. Eisch and B. W. Kotowicz, *Eur. J. Inorg. Chem.*, 1998, 761–769.
- 30 W. J. Scott, G. T. Crisp and J. K. Stille, *Org. Synth.*, 1990, **68**, 116.
- 31 An analogous phenomenon has already been observed for mixtures of certain N- or P-ligands and B- or In-Lewis acids: (a) M. Fontani, F. Peters, W. Scherer, W. Wachter, M. Wagner and P. Zanello, *Eur. J. Inorg. Chem.*, 1998, 1453–1465; (b) ref. 16; (c) M. Grosche, E. Herdtweck, F. Peters and M. Wagner, *Organometallics*, 1999, **18**, 4669–4672; (d) R. E. Dinnebier, M. Wagner, F. Peters, K. Shankland and W. I. F. David, *Z. Anorg. Allg. Chem.*, 2000, **626**, 1400–1405; (e) M. Scheibitz, J. W. Bats, M. Bolte and M. Wagner, *Eur. J. Inorg. Chem.*, 2003, 2049–2053; (f) M. Scheibitz, M. Bolte, H.-W. Lerner and M. Wagner, *Organometallics*, 2004, **23**, 3556–3559.
- 32 A. Lorbach, M. Bolte, H.-W. Lerner and M. Wagner, *Chem. Commun.*, 2010, **46**, 3592–3594.
- 33 (i) The addition of monodentate pyridine (2 equiv.) also releases (2)₂. However, the AlBr₃/py adduct(s) that are formed as byproduct(s) remain soluble and are therefore difficult to remove. (ii) Adding 2 equiv. bipy to 2·(AlBr₃)₂ results in the precipitation of all Al-containing compounds (in C₆D₆); the ¹H NMR spectrum of the supernatant shows no resonances, except for the solvent signal. (iii) As control experiments, we have also prepared 2:1 and 1:1 mixtures of AlBr₃ and bipy in C₆D₆. In both cases, a precipitate formed; the supernatants showed either no bipy signals (2:1 mixture) or significant bipy signals (1:1 mixture). NMR analysis of each precipitate in CD₃CN displayed a strong resonance at δ(²⁷Al) = 81.0 ppm, assignable to the [AlBr₄][−] anion (literature value: 80.0 ppm as taken from: J. W. Akitt, Aluminum, Gallium, Indium, and Thallium, in *Multinuclear NMR*, ed. J. Mason, Plenum Press, New York, 1987, ch. 9, p. 269. The ¹H resonance patterns of both precipitates were essentially identical, though rather complex, indicating the presence of various bipy-containing cations. Overall, the NMR characteristics of the precipitate that had been isolated (in quantitative yield) during the synthesis of (2)₂ are comparable to those observed in the control experiments. For an earlier study of the AlBr₃/bipy system, see: J. Y. Corey and R. Lamberg, *Inorg. Nucl. Chem. Lett.*, 1972, **8**, 275–280.
- 34 V. C. Williams, W. E. Piers, W. Clegg, M. R. J. Elsegood, S. Collins and T. B. Marder, *J. Am. Chem. Soc.*, 1999, **121**, 3244–3245.
- 35 Deposition Numbers 2385628 (for (1)₂), 2385629 (for 1·(py)₂), 2385630 (for K[1·(μ-pz)]), 2385631 (for 1·(pyz)(thf)), 2385632 (for DAA-R₂·(AlBrR₂)₂ (R = Me or Br)), 2385633 (for α-2·(AlBr₃)₂), 2385634 (for β-2·(AlBr₃)₂), 2385635 (for (2)₂), 2385636 (for 2·(thf)₂), 2385637 (for 2·(py)₂), 2385638 (for [nBu₄N][3]), 2385639 (for 1·(thf)₂), and 2385640 (for 2·(OEt₂)₂) contain the ESI[†] crystallographic data for this paper. These data are provided free of charge by the joint Cambridge Crystallographic Data Centre and Fachinformationszentrum Karlsruhe Access Structures service.
- 36 C. A. Reed, K.-C. Kim, E. S. Stoyanov, D. Stasko, F. S. Tham, L. J. Mueller and P. D. W. Boyd, *J. Am. Chem. Soc.*, 2003, **125**, 1796–1804.
- 37 (a) H. Schnöckel, M. Leimkühler, R. Lotz and R. Mattes, *Angew. Chem., Int. Ed.*, 1986, **25**, 921–922; (b) R. Ahlrichs, M. Häser, H. Schnöckel and M. Tacke, *Chem. Phys. Lett.*, 1989, **154**, 104–110; (c) C. Üffing, A. Ecker, R. Köppe, K. Merzweiler and H. Schnöckel, *Chem.–Eur. J.*, 1998, **4**, 2142–2147.
- 38 Donor adducts of 1,4-dialuminacyclohexadienes have been prepared by Hoberg *et al.* through the cyclocondensation of Na₂[*cis*-(Et₃Al)(Ph)C=C(Ph)(AlEt₃)] or *via* photochemical reactions: (a) H. Hoberg, V. Gotor, A. Milchereit, C. Krüger and J. C. Sekutowski, *Angew. Chem., Int. Ed.*, 1977, **16**, 539; (b) H. Hoberg and F. Aznar, *J. Organomet. Chem.*, 1979, **164**, C13–C15; (c) H. Hoberg and F. Aznar, *J. Organomet. Chem.*, 1980, **193**, 161–163.
- 39 To facilitate the structure discussion, we will from now on treat (1)₂^A as if it had an exact D_{2d} symmetry in the solid state.
- 40 R. G. Vranka and E. L. Amma, *J. Am. Chem. Soc.*, 1967, **89**, 3121–3126.



- 41 D. D. Eley, J. H. Taylor and S. C. Wallwork, *J. Chem. Soc.*, 1961, 3867–3873.
- 42 A. Lorbach, M. Bolte, H. Li, H.-W. Lerner, M. C. Holthausen, F. Jäkle and M. Wagner, *Angew. Chem., Int. Ed.*, 2009, **48**, 4584–4588.
- 43 A. Nangia, Molecular Conformation and Crystal Lattice Energy Factors in Conformational Polymorphs, in *Models, Mysteries and Magic of Molecules*, ed. J. C. A. Boeyens and J. F. Ogilvie, Springer, Dordrecht, 2008, ch. 3, pp. 63–86.
- 44 The compound $2 \cdot (\text{AlBr}_3)_2$ crystallizes in two polymorphous modifications that differ by the number of crystallographically unique molecules (two molecules in the denser α -form and one in the less dense β -form). Since the geometrical characteristics of the molecules are similar, we are focusing here on the β -form. More details are provided in the ESI.†
- 45 W. Zheng, A. Stasch, J. Prust, H.-W. Roesky, F. Cimpoesu, M. Noltemeyer and H.-G. Schmidt, *Angew. Chem., Int. Ed.*, 2001, **40**, 3461–3464.
- 46 Selected examples of bicyclic compounds $[\text{RAl}(\mu\text{-}3,5\text{-}t\text{Bu}_2\text{pz})_2(\mu\text{-E})\text{AlR}]$: (a) R = H, E = O–Te: W. Zheng, N. C. Mösch-Zanetti, H.-W. Roesky, M. Noltemeyer, M. Hewitt, H.-G. Schmidt and T. R. Schneider, *Angew. Chem., Int. Ed.*, 2000, **39**, 4276–4279; (b) R = PhCC, E = S–Te: W. Zheng, H. Hohmeister, N. C. Mösch-Zanetti, H.-W. Roesky, M. Noltemeyer and H.-G. Schmidt, *Inorg. Chem.*, 2001, **40**, 2363–2367.
- 47 Boron-containing heterotriptycenes are known: (a) ref. 32; (b) Ö. Seven, S. Popp, M. Bolte, H.-W. Lerner and M. Wagner, *Dalton Trans.*, 2014, **43**, 8241–8253; (c) A. Ben Saida, A. Chardon, A. Osi, N. Tumanov, J. Wouters, A. I. Adjieufack, B. Champagne and G. Berionni, *Angew. Chem., Int. Ed.*, 2019, **58**, 16889–16893; (d) A. Chardon, A. Osi, D. Mahaut, T.-H. Doan, N. Tumanov, J. Wouters, L. Fusaro, B. Champagne and G. Berionni, *Angew. Chem., Int. Ed.*, 2020, **59**, 12402–12406; (e) A. Osi, D. Mahaut, N. Tumanov, L. Fusaro, J. Wouters, B. Champagne, A. Chardon and G. Berionni, *Angew. Chem., Int. Ed.*, 2022, **61**, e202112342; (f) M. Henkelmann, A. Omlor, M. Bolte, V. Schünemann, H.-W. Lerner, J. Noga, P. Hrobárik and M. Wagner, *Chem. Sci.*, 2022, **13**, 1608–1617; (g) A. Osi, N. Tumanov, J. Wouters, A. Chardon and G. Berionni, *Synthesis*, 2023, **55**, 347–353; (h) S. E. Prey, J. Gilmer, S. V. Teichmann, L. Čaić, M. Wenisch, M. Bolte, A. Virovets, H.-W. Lerner, F. Fantuzzi and M. Wagner, *Chem. Sci.*, 2023, **14**, 5316–5322.
- 48 (a) C.-C. Chang, T.-Y. Her, F.-Y. Hsieh, C.-Y. Yang, M. Y. Chiang, G.-H. Lee, Y. Wang and S.-M. Peng, *J. Chin. Chem. Soc.*, 1994, **41**, 783–789; (b) J. Lewiński, J. Zachara, T. Kopeć, I. Madura and I. Prowotorow, *Inorg. Chem. Commun.*, 1999, **2**, 131–134.
- 49 (a) F. Bickelhaupt, *Angew. Chem., Int. Ed.*, 1987, **26**, 990–1005; (b) F. Bickelhaupt, *Pure Appl. Chem.*, 1990, **62**, 699–706.
- 50 G. Wittig and F. Bickelhaupt, *Chem. Ber.*, 1958, **91**, 883–894.
- 51 N. A. A. Al-Jabar and A. G. Massey, *J. Organomet. Chem.*, 1984, **275**, 9–18.
- 52 H. J. S. Winkler and G. Wittig, *J. Org. Chem.*, 1963, **28**, 1733–1740.
- 53 M. S. Goedheijt, T. Nijbacker, O. S. Akkerman, F. Bickelhaupt, N. Veldman and A. L. Spek, *Angew. Chem., Int. Ed.*, 1996, **35**, 1550–1552.
- 54 A. Lorbach, C. Reus, M. Bolte, H.-W. Lerner and M. Wagner, *Adv. Synth. Catal.*, 2010, **352**, 3443–3449. A simplified version of this published protocol, which we refer to here, can be found in the ESI.†
- 55 The reaction of $[\text{nBu}_4\text{N}][3]$ with Me_2SiCl_2 or Me_3SnCl gives 9,9,10,10-tetramethyl-9,10-dihydro-9,10-disilaanthracene or 1,2-(Me_2BrSn) $_2\text{C}_6\text{H}_4$, respectively. These reactions are not yet optimized and represent the onset of an investigation into the full scope of the reaction, which will be reported at a later stage.

